BIOCHEMISTRY
including biophysical chemistry & molecular biology

Article

pubs.acs.org/biochemistry

Antiproliferative Effect of pHLIP-Amanitin

Anna Moshnikova, Valentina Moshnikova, Oleg A. Andreev, and Yana K. Reshetnyak*

Physics Department, University of Rhode Island, 2 Lippitt Road, Kingston, Rhode Island 02881, United States

ABSTRACT: Toxins could be effective anticancer drugs, if their selective delivery into cancer cells could be achieved. We have shown that the energy of membrane-associated folding of water-soluble membrane peptides of the pHLIP (pH low insertion peptide) family could be used to move cell-impermeable cargo across the lipid bilayer into the cytoplasm of cancer cells. Here we present the results of a study of pHLIP-mediated cellular delivery of a polar cell-impermeable toxin, α-amanitin, an inhibitor of RNA polymerase II. We show that pHLIP can deliver α-amanitin into cells in a pH-dependent fashion and induce cell death within 48 h. Translocation capability could be tuned by conjugating amanitin to the C-terminus of pHLIP via linkers of different hydrophobicities that could be cleaved in the cytoplasm. pHLIP-SPDP-amanitin, which exhibits 4−5 times higher antiproliferative ability at pH 6 than at pH 7.4, was selected as the best construct. The major mechanism of amanitin delivery is direct translocation (flip) across a membrane by pHLIP and cleavage of the S−S bond in the cytoplasm. The antiproliferative effect was monitored on four different human cancer cell lines. pHLIP-mediated cytoplasmic delivery of amanitin could create great opportunities to use the toxin as a potent pH-selective anticancer agent, which predominantly targets highly proliferative cancer cells at low extracellular pH values.

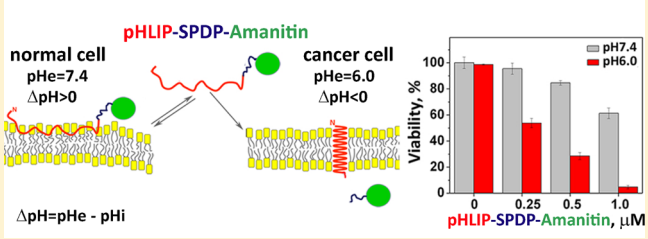

One of the main goals of cancer treatment is to kill cancer cells without affecting cells in healthy tissues and organs. A number of toxic compounds have been tested; however, the side effects have been significant. Therefore, therapeutic use of these compounds is limited unless they can be delivered specifically to cancer cells. If the target of a polar therapeutic is cytoplasmic, the selective delivery of therapeutics to a tumor is not sufficient to improve treatment; it is necessary to move the drug molecule across cellular membrane and release it inside the cell. Over the past several decades, various nanocarriers were introduced for encapsulation of therapeutic payloads and delivery to tumors if tumor targeting molecules decorate nanocarriers.[1,2] The mechanism of cellular entry of nanocarriers is predominantly endocytotic, which leads to the trapping of therapeutic molecules in endosomes. pH-sensitive functionalities could be incorporated into nanocarriers to promote disruption of endosomal membranes and facilitate the release of the payload into the cytoplasm.[3−7] We are developing a new approach for direct cytoplasmic delivery of polar cargo. Our concept is based on utilization of the energy of membrane-associated folding of family of pHLIPs (pH low insertion peptides) for the pH-dependent translocation of cell-impermeable molecules across the plasma membrane into the cytoplasm.[8] We demonstrate targeting of acidic solid tumors by pHLIP peptides labeled with fluorescent, PET, and SPECT imaging agents, delivery of gold nanoparticles and liposomes to acidic diseased tissue, and cytoplasmic delivery of various cell-impermeable molecules.[9−16] Among functional cargo molecules tested for intracellular delivery by pHLIP were bicyclic heptapeptides, mushroom phallotoxins.[8,17] The toxins were translocated into cultured cells in a pH-dependent manner, released into the cytoplasm by cleavage of the S−S bond, and bound to an intracellular target, F-actin. Phallatoxins delivered to cells by pHLIP induced stabilization of cell cytoskeleton, which led to cell death. We show that hydrophobicity of phallotoxin cargo could be tuned to enhance translocation.[18] The objective of this study is an evaluation of the ability of pHLIP to translocate another mushroom toxin, bicyclic octapeptide α-amanitin. Despite the similarity in chemical structure between phallo and amanita toxins, they possess very different biological activities.[19−21] Amanitin is an inhibitor of RNA polymerase II, inhibition of which blocks protein synthesis and induces cell death.[22] This toxin could be considered as a potent anticancer drug if it could be specifically delivered to the cytoplasm of cancer cells. Here we demonstrate that pHLIP can deliver α-amanitin into cells in a pH-dependent fashion and induce cell death within 48 h.

MATERIALS AND METHODS

Materials and Peptide Preparation. α-Amanitin, 4′,6-diamidino-2-phenylindole (DAPI), and propidium iodine (PI) were purchased from Sigma-Aldrich. *N*-Succinimidyl 3-(2-pyridyldithio)propionate (SPDP), sulfosuccinimidyl 6-[α-methyl-α-(2-pyridyldithio)toluamido]hexanoate (sulfo-Lc-SMPT), and *N*-(α-maleimidoacetoxy)succinimide ester (AMAS) were from Thermo Scientific. 6-(Fluorescein-5-carboxamido) hexanoic acid, succinimidyl ester (5-SFX) was from Invitrogen, and anexinV-FITC was from BD Biosciences. The pHLIP peptides with a single Cys at the C- or N-terminus (pHLIP-Cys, AEQNPIYWARYADWLFTTPLLLLDLALLVDADEGCT; and

Received: December 10, 2012
Revised: January 28, 2013
Published: January 29, 2013

   dx.doi.org/10.1021/bi301647y | *Biochemistry* 2013, 52, 1171−1178

Cys-pHLIP, ACEQNPIYWARYADWLFTTPLLLLDLALLVD-ADEGT) were synthesized and purified by J. I. Elliott at the W. M. Keck Foundation Biotechnology Resources Laboratory at Yale University (New Haven, CT).

Conjugation of Amanitin to pHLIP. First, amanitin was conjugated with a cross-linker (cleavable SPDP, sulfo-Lc-SMPT, or noncleavable, AMAS). Amanitin was incubated at room temperature for 4 h with a 10-fold excess of cross-linker in 50 mM sodium phosphate buffer (pH 7.6) containing 150 mM sodium chloride followed by purification of the products by reverse phase HPLC. Next, Cys-pHLIP or pHLIP-Cys peptide was incubated with SPDP-amanitin, Lc-SMPT-amanitin, or AMAS-amanitin in 100 mM sodium phosphate buffer (pH 7.8, saturated with argon) containing 150 mM sodium chloride at a ratio of 1:1 at room temperature for 1 h. The final products were purified by reverse phase HPLC, lyophilized, and characterized by SELDI-TOF mass spectrometry. The concentration of constructs was determined by the absorbance of amanitin at 310 nm using a molar extinction coefficient of 13000 M^{-1} cm^{-1}.

Synthesis of Amanitin-SFX. Amanitin was incubated with 6-(fluorescein-5-carboxamido)hexanoic acid, succinimidyl ester (SFX) in 50 mM sodium phosphate, 150 mM sodium chloride buffer (pH 7.6) at a ratio 1:5 at room temperature for 4 h followed by purification of the product by reverse phase HPLC and characterized by SELDI-TOF mass spectrometry.

Measurements of the Water−Octanol Partition Coefficient. The polarity of amanitin and amanitin conjugated to the SPDP or Lc-SMPT cross-linkers was determined by the assessment of relative partitioning between aqueous and octanol liquid phases. Constructs dissolved in a 1:1 MeOH/water mixture were added to 0.5 mL of 10 mM phosphate buffer (pH 7.4, saturated with argon), followed by the addition of argon-saturated *n*-octanol (0.5 mL), and sealed under argon. The solutions were mixed by rotation for 24 h at room temperature and left for an additional 24−48 h for equilibration. After phase separation, the absorption at 300 nm was recorded. Molar extinction coefficients in *n*-octanol and phosphate buffer are assumed to be the same, and the ratio of the OD readings was used directly to calculate the partition coefficient ($P = OD_{n\text{-octanol}}/OD_{water}$) and log *P* values.

Liposome Preparations. Liposomes were prepared by extrusion. POPC (1-palmitoyl-2-oleoyl-*sn*-glycero-3-phosphocholine) was transferred to a round-bottom flask, and a lipid layer was obtained by evaporating the chloroform in a rotary evaporator, followed by drying under high vacuum for 2 h. The lipid layer was resuspended in 10 mM phosphate buffer (pH 8) and extruded 31 times through a 100 nm membrane to yield large unilamellar vesicles.

Steady-State Fluorescence and Circular Dichroism Measurements. Intrinsic peptide fluorescence and circular dichroism (CD) spectra were measured on a PC1 ISS spectrofluorometer (ISS, Inc.) and a MOS-450 spectrometer (Biologic, Inc.), respectively. All measurements were performed at 25 °C. Samples of 2 μM pHLIP-SPDP-Am and pHLIP-Lc-SMPT-Am incubated overnight in the presence or absence of 2 mM POPC in pH 8 phosphate buffer were used for the measurements of CD and fluorescence signals of states I and II. State I is the peptide in solution at pH 8; state II is the peptide in the presence of POPC liposomes at pH 8, and state III reflects folding and insertion of the peptide into a lipid bilayer of liposomes and formation of a transmembrane helix, when the pH is decreased from 8 to 3.6 by addition of an aliquot of 0.1 M HCl. Peptide fluorescence spectra were recorded from 310 to 400 nm using an excitation wavelength of 280 nm. Peptide CD spectra were recorded from 190 to 260 nm in 0.5 nm increments using a sample cuvette with an optical path length of 0.5 cm.

pH Dependence. pH-dependent partitioning of pHLIP-SPDP-Am into the lipid bilayer was investigated by the shift in the position of the peptide intrinsic fluorescence spectral maximum for the pHLIP induced by a decrease in pH from 8 to 3 by the addition of HCl in the presence of POPC liposomes. A 2 μM peptide solution was incubated overnight with 2 mM POPC liposomes, and the pH was decreased by the addition of aliquots of 0.1 M HCl. The resulting pH values were measured using a microelectrode probe (Thermo Electron Corp., Orion Ross Micro pH electrode). Fluorescence spectra were recorded at each pH value. The spectra were analyzed with decomposition algorithms using an online PFAST toolkit [Protein Fluorescence And Structural Toolkit (http://pfast.phys.uri.edu/[23])] to obtain spectral maxima (λ_{max}). Finally, the positions of the fluorescence spectral maxima (λ_{max}) of the single-component solutions were plotted versus pH, and the Henderson−Hasselbalch equation was used to fit the data:

$$\lambda_{max} = \lambda_{2max} + \frac{\lambda_{1max} - \lambda_{2max}}{1 + 10^{pH-pK_a}}$$

where λ_{1max} and λ_{2max} are fluorescence maximal wavelengths at the beginning and end of the transition, respectively, and pK_a is the midpoint of the transition. It is assumed that there is a linear relation between the position of the maximum and the contribution of state II (or state III). However, because quantum yields in states II and III are slightly different, there was a slight nonlinearity. According to our previous estimation, the apparent p*K* shifts no more than 0.05 pH unit toward lower pH values if quantum yields of states II and III are taken into account.[24] Because this shift is smaller than the experimental error, we present the pK_a values for transitions from state II to state III based on the analysis of the positions of spectral maxima and assuming that quantum yield is the same in states II and III.

Cell Lines. Human cervix adenocarcinoma (HeLa) cells, human osteosarcoma (U2OS) cells, human breast ductal carcinoma M4A4 cells, and human breast adenocarcinoma MDA-MB-231 cells were acquired from American Type Culture Collection. Human cervix adenocarcinoma cells with stable expression of green fluorescent protein (GFP) (HeLa-GFP cells) was acquired from the Cell Biolabs Inc. Cells were authenticated, stored according to the supplier's instructions, and used within 3 months after frozen aliquot resuscitations. Cells were cultured in Dulbecco's modified Eagle's medium (DMEM) supplemented with 10% fetal bovine serum (FBS) and 10 μg/mL ciprofloxacin in a humidified atmosphere of 5% CO_2 and 95% air at 37 °C. The pH 6.0 medium was prepared by mixing 13.3 g of dry DMEM in 1 L of deionized water.

Fluorescence Microscopy. HeLa-GFP and HeLa cells were grown in 35 mm dishes with 14 mm glass-bottom windows coated with collagen. Cells were transferred to DMEM at pH 6.5 or 7.4 followed by incubation with 0.5−1 μM pHLIP-S-S-amanitin at the same pH values for 2 h. Control cells were treated with 1 μM staurosporine for 4 h. After the cells had been treated, the construct was removed and cells were transferred to the standard growth medium. At various time points, cells were stained with 5 μg/mL DAPI or 2 μg/mL PI for 20 min or Annexin V-FITC according to the

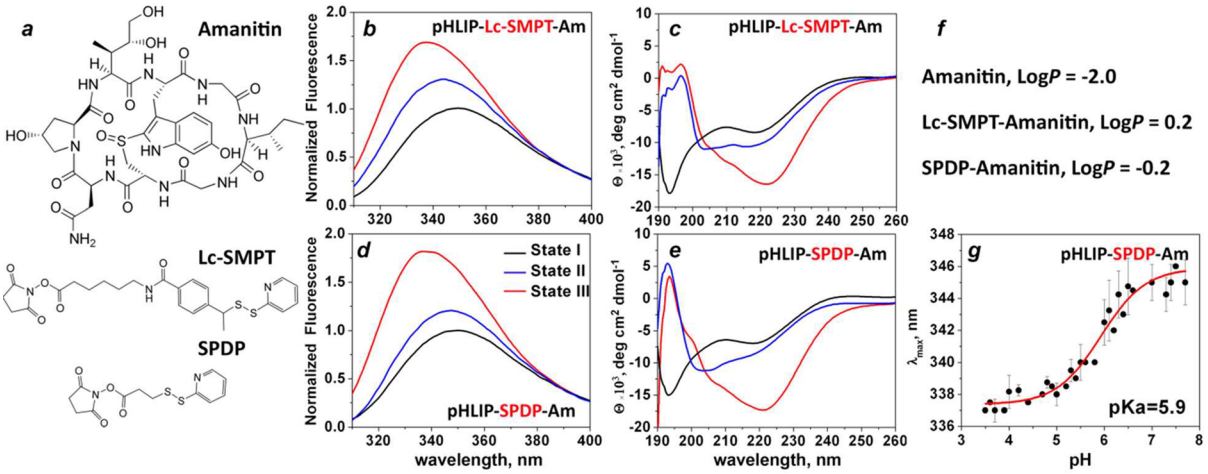

Figure 1. Interaction of pHLIP-amanitin with the lipid bilayer of liposomes. (a) Chemical structure of amanitin and long-chain (Lc-SMPT) and short-chain (SPDP) cross-linkers. (b–e) Fluorescence (b and d) and CD (c and e) spectra representing three states of pHLIP-amanitin conjugated via long-chain, SMPT (b and c), and short-chain, SPDP (d and e), cross-linkers. State I corresponds to the construct in aqueous solution at pH 8; addition of liposomes results in the formation of state II, and state III represents the peptide inserted into the lipid bilayer at pH 4. (f) Log *P* values of amanitin and its conjugates with long- and short-chain cross-linkers (where *P* is the octanol–water partition coefficient). (g) pH dependence of the pHLIP-SPDP-Am transition from state II to state III.

manufacturer's instructions followed by intensive washing. Fluorescent and phase-contrast images of the cells were acquired with a Retiga CCD camera (Q-imaging) mounted onto the inverted Olympus IX71 microscope (Olympus America, Inc.). To monitor the changes in cell morphology in real time after treatment with pHLIP-S-S-amanitin, dishes with cells were placed in a live cell imaging chamber (Tokai Hit).

Proliferation Assay. HeLa, U2OS, M4A4, or MDA-MB-231 cells were loaded in the wells of 96-well plates (~5000 cells per well) and incubated overnight. Growth medium was replaced with medium without FBS at pH 6.0 or 7.4 containing increasing amounts of constructs (0.125, 0.25, 0.5, 1, and up to 10 μM for amanitin and amanitin-SFX). In most cases, treatment was performed in DMEM at pH 6.0 and 7.4, while in the case of pHLIP-Lc-SMPT-amanitin, treatment was performed in PBS at pH 6.2 or 8.0. After the cells had been treated for 2 h, the constructs were removed and replaced with standard growth medium containing 10% FBS. Cell viability was assessed by a colorimetric reagent (CellTiter 96 AQ_{ueous} One Solution Assay, Promega), which was added for 1 h to cells followed by the measurement of absorbance at 490 nm. All samples were prepared in triplicate. Each experiment was repeated at least three times.

ECIS Assay. The kinetics of inhibition of proliferation of HeLa-GFP cells treated with pHLIP-SPDP-Am at pH 6.5 were monitored by changes of capacitance measured at AC frequencies on an ECIS 8Z (electric cell-substrate impedance sensing) instrument (Applied Biophysics, Inc.). Cells (~5000 cells per well) were loaded in an 8W10E+ eight-well plate (Applied Biophysics, Inc.) and incubated overnight. Each well had two sets of 20 circular 250 μm diameter active gold electrodes. Growth medium was replaced with the medium without FBS at pH 6.0 or 7.4 containing 0.5 μM pHLIP-SPDP-amanitin or amanitin alone. The constructs were removed after the cells had been treated for 2 h, and the cells were incubated in standard growth medium for 60 h. Changes in capacitance were monitored for 50 h after the treatment. The time of the treatment was set as zero.

RESULTS

Biophysical Characterization of the Interaction of pHLIP-Amanitin with the Membrane. A bicyclic peptide, amanitin, containing a reactive NH_2 group was conjugated with the C-terminus of pHLIP via a cleavable S–S bond by two cross-linkers of different polarity: long-chain hydrophobic Lc-SMPT and short-chain, more polar SPDP (Figure 1a). The three states of pHLIP-amanitin constructs were monitored by changes in peptide fluorescence excited at 280 nm (Figure 1b,d) and circular dichroism (Figure 1c,e) spectral signals. State I represents the construct in aqueous solution at pH 8; addition of liposomes results in the transition to state II, where the pHLIP peptide is in equilibrium between membrane-bound and free forms, and state III reflects insertion of the peptide into the lipid bilayer and formation of a transmembrane helix as the result of a decrease in pH from 8 to 4.[25] The nonphysiological pH values of 8 and 4 were selected to ensure the completion of the transition in this model experiment on liposomes. Both constructs show pH-dependent interaction with the lipid bilayer of the membrane. However, at pH 8 in the presence of liposomes (state II, blue lines in Figure 1), the amount of membrane-inserted form is larger for pHLIP-Lc-SMPT-Am than for pHLIP-SPDP-Am. This is reflected by a 3 nm shift of the position of the maximal of the fluorescence spectrum to short wavelengths (λ_{max} values of pHLIP-SPDS-Am and pHLIP-Lc-SMPT-Am in state II of 347 and 344 nm, respectively), an 11% increase in the magnitude of the fluorescence signal, and a decrease in the molar ellipticity at 220 nm (Θ values of pHLIP-Lc-SMPT-Am and pHLIP-Lc-SMPT-Am in state II of 6.8–8.3 × 10^3 deg cm^2 $dmol^{-1}$). It could be explained by the difference in the hydrophobicity of the amanitin cargo conjugated to the two different cross-linkers. Conjugation of the polar membrane-impermeable amanitin [log *P* ~ −2 (Figure 1f)] to the cross-linkers reduces the polarity of the constructs (log *P* of amanitin-SPDP of approximately −0.2) and converts amanitin-Lc-SMPT cargo to slightly membrane permeable (positive log *P* value of 0.2), which results in the higher affinity of pHLIP-Lc-SMPT-Am for the lipid bilayer of the membrane already at pH 8. The cell

dx.doi.org/10.1021/bi301647y | *Biochemistry* 2013, 52, 1171–1178

experiments were mostly performed with pHLIP-SPDP-Am, which has an apparent p*K* of insertion into the membrane equal to 5.9, similar to that of the pHLIP peptide alone and the pHLIP conjugated to phallatoxin and biotin cargoes.[18,24,26]

Inhibition of Cell Proliferation. Amanitin is a potent inhibitor of RNA polymerase II, which, once translocated into cells, induces their death. Amanitin is a polar molecule and cannot freely diffuse across the membrane, especially at low concentrations. The ability of pHLIP to move amanitin across the membrane and to inhibit cell proliferation in concentration- and pH-dependent manners was evaluated on several cancer cell lines (Figure 2). The time of incubation of constructs with cells was varied, and the cytotoxic effect was evaluated using the standard MTS assay at various time points. All data presented here were obtained after incubation of the constructs with cells for 2 h, followed by the removal of the constructs and transfer of the cells to standard cell growth medium. Cell death was monitored 48 h after the treatment.

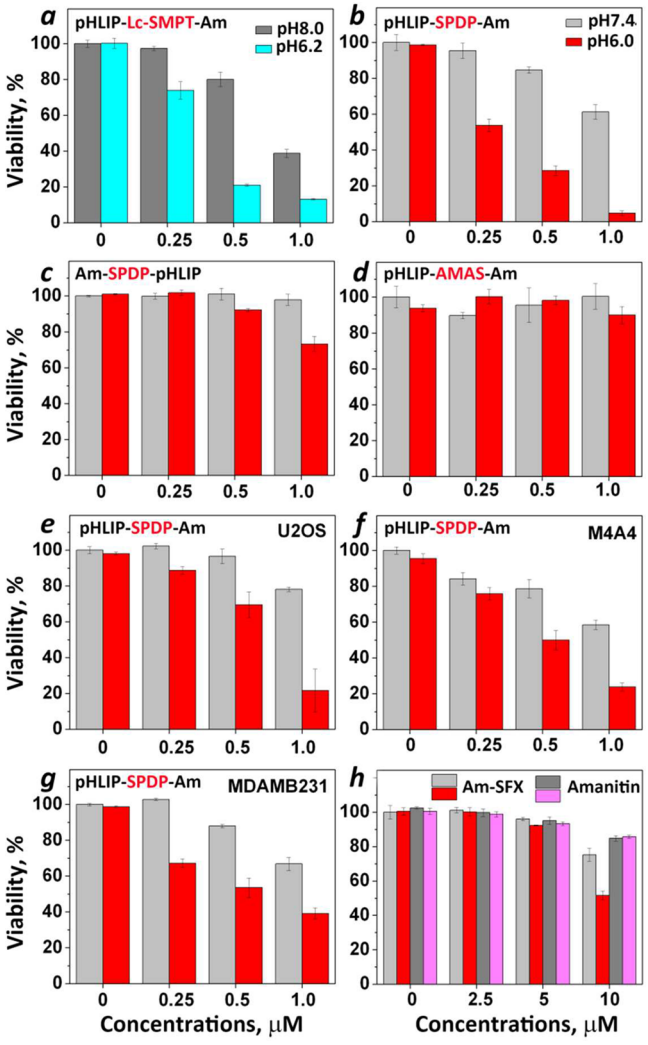

Figure 2. Inhibition of cell proliferation. Human cervix adenocarcinoma, HeLa-GFP (a–d and h) human osteosarcoma, U2OS (e), human breast ductal carcinoma M4A4 (f), and human breast adenocarcinoma MDA-MB-231 (g) cells were treated with the following constructs: pHLIP-Lc-SMPT-Am (a), pHLIP-SPDP-Am (b and e–g), Am-SPDP-pHLIP (c), pHLIP-AMAS-AM (d), and amanitin-SFX and amanitin alone (h) for 2 h in DMEM at normal and high pH (light and dark gray columns, respectively) or low pH (pH 6.2, blue column, and pH 6.0, red and magenta columns) followed by the removal of the constructs and the transfer of cells to standard cell growth medium. The MTS assay was performed 48 h after the treatment. Amanitin and pHLIP alone have no effect on the proliferation of all investigated cell lines at both pH values (data not shown).

pH-dependent inhibition of the proliferation of HeLa cells treated with pHLIP-Lc-SMPT-Am was observed only when the treatment was performed in PBS at pH 8 (Figure 2a), because at neutral pH the cytotoxic effect was just slightly less compared to that caused by the low-pH treatment (data not shown). At the same time, the cytotoxic effect of pHLIP-SPDP-Am was significantly lower at pH 7.4, while at pH 6.0, concentration-dependent cell death was observed (Figure 2b). Cells treated with amanitin conjugated to the N-terminus of pHLIP (Am-SPDP-pHLIP) show slight toxicity at low pH at a concentration of 1 μM (Figure 2c), which might be associated with partial endocytotic uptake of the construct by the cells promoted by interaction of pHLIP with the plasma membrane at low pH or the possibility of the insertion of some population of the peptide into the cellular membrane translocating the N-terminus across a bilayer. The cytotoxic effect after the cells had been treated with Am-SPDP-pHLIP was much smaller than the effect after the cells had been treated with pHLIP-SPDP-Am. Another control experiment was performed with amanitin conjugated to the C-terminus of pHLIP via a noncleavable cross-linker, AMAS, with a polarity similar to that of SPDP (pHLIP-AMAS-Am). No cellular toxicity was observed at either pH over a wide range of concentrations (Figure 2d), which confirms that amanitin needs to be released from the peptide to diffuse to the nucleus and find its target.

Treatment of various cancer cell lines, including human osteosarcoma (U2OS), breast ductal carcinoma (M4A4), and breast adenocarcinoma (MDA-MB-231), with pHLIP-SPDP-Am led to the inhibition of cell proliferation in concentration- and pH-dependent manners (Figure 2e–g). All cells were also treated with amanitin alone, and no toxicity was observed (data not shown).

Besides the testing of the pHLIP-based constructs, we evaluated the cytotoxic effect of amanitin conjugated with fluorescein-hexanoic acid (SFX), which contains a protonatable carboxyl group, and hexanoic acid for the enhancement of the affinity of the construct for the membrane. Some pH-dependent toxic effect was observed only at concentrations (10 μM) 10 times higher than what was needed for the inhibition of cell proliferation by pHLIP-SPDP-Am (Figure 2h).

Kinetics of Inhibition of Cell Proliferation. The kinetics of inhibition of proliferation of HeLa-GFP cells treated with pHLIP-SPDP-Am at pH 6.5 were monitored by the changes in capacitance measured at AC frequencies using ECIS (Figure 3a). Capacitance varies in a linear fashion with the fractional cell coverage of the bottom of a special chamber coated with thin film gold electrodes connected to the ECIS electronics.[27] When cells are shrinking and dying after being treated with pHLIP-SPDP-Am, the capacitance increases, reaching saturation 40–50 h after the treatment. Changes in cell morphology were also observed on the optical microscope connected to the live-cell chamber (Figure 3b–f). In accordance with the capacitance measurements, the changes in cell morphology (rounding of the cells) were completed at 49 h.

Mechanism of Cell Death. To evaluate the mechanism of cell death induced by pHLIP-SPDP-Am, we monitored the

dx.doi.org/10.1021/bi301647y | *Biochemistry* 2013, 52, 1171–1178

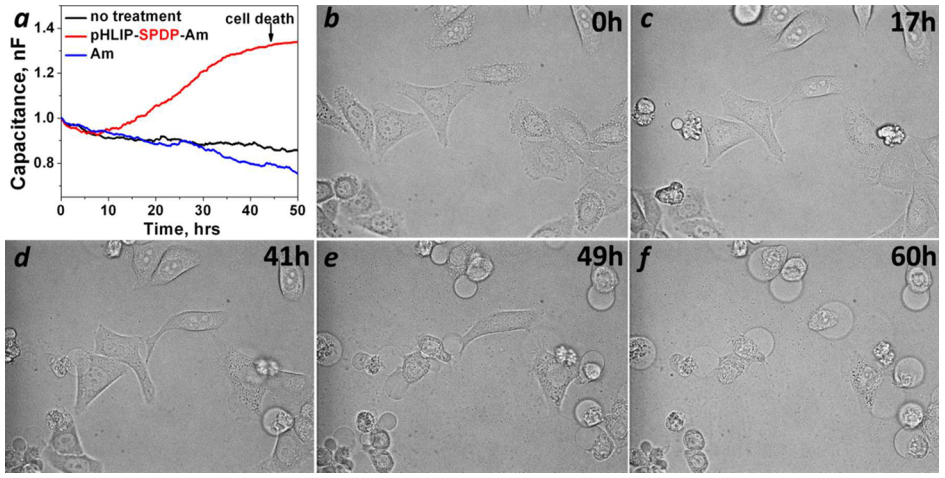

Figure 3. Time course of inhibition of cell proliferation. HeLa-GFP cells were treated with pHLIP-SPDP-Am for 2 h in DMEM at pH 6.5 followed by the removal of the construct (zero time point) and the transfer of cells to the standard growth medium. The kinetics of inhibition of cell proliferation were monitored by changes in capacitance (a) and cell morphology (b–f).

appearance of phosphatidylserine on the outer surface of the plasma membrane and the DNA fragmentation, which are signs of early apoptosis. Nontreated HeLa cells and cells treated with pHLIP-SPDP-Am and staurosporine, which is known to induce apoptosis in HeLa cells,[28,29] were stained with cell-impermeable phosphatidylserine-binding protein, Annexin V-FITC. The plasma membrane of cells at 4 h after they had been treated with staurosporine was stained with Annexin V-FITC (Figure 4e), while the integrity of the membrane was not compromised in most cases, because cell-impermeable DNA staining dye, PI, was not able to label the cellular nucleus (Figure 4f). Despite the fact that 11 h after the treatment with pHLIP-SPDP-Am some cells had already undergone morphological changes (Figure 4a), we did not observe the appearance of the phosphatidylserine on the outer leaflet of the plasma membrane. Another sign of early apoptosis, DNA fragmentation, was evaluated on HeLa cells at various time points (5, 8, 11, 14, and 17 h) after treatment with pHLIP-SPDP-Am by staining the cells with the membrane-impermeable DNA binding dye, DAPI. The cells at selected time points after the treatment are shown in Figure 4j–o. With the progression of time, the number of cells with a changed morphology (Figure 4j,l,n, shown with asterisks) was increasing, while the DNA fragmentation was occurring only in a small population (Figure 4k,m,o, shown with arrows). We concluded that the major pathway of cell death after pHLIP-SPDP-Am treatment is necrotic; however, we cannot exclude the possibility that apoptotic pathway could also be triggered in some subset of cells.

DISCUSSION

α-Amanitin belongs to the class of strong toxins and can induce cell death within 48 h. However, it is too polar to cross the cellular membrane by itself, except that of liver cells, which have a special transporting system for the uptake of small cyclic molecules like phallo and amanita toxins.[30] Amanitin could be considered as a potent anticancer drug if it could be delivered only to cancer cells and translocated across the membrane. Recently, the antiproliferative effect of α-amanitin conjugated with the anti-EpCAM antibody was tested on human cancer cell lines and assessed in vivo in immune-compromised mice bearing subcutaneous human pancreatic carcinoma xenograft tumors.[31] The study suggested that anti-EpCAM antibody conjugates with α-amanitin have the potential to be highly effective therapeutic agents for pancreatic carcinomas and various EpCAM-expressing malignancies. Here we tested the ability of a novel pHLIP-based drug delivery system to translocate α-amanitin across the membrane into the cytoplasm. This system is based on a pH-dependent spontaneous insertion and folding of the pHLIP peptide in the membrane. The molecular mechanism of the action of pHLIPs is a protonation of Asp/Glu residues in a mildly acidic environment, which leads to the increase in the hydrophobicity of the peptide and promotes peptide insertion and folding in the membrane. It is important to outline that in contrast to normal cells, cancer cells have a negative transmembrane pH gradient (extracellular pH lower than intracellular pH), which promotes accumulation of weak acids in cancer cells.[32,33] Thus, in cancer cells, the equilibrium is shifted toward the pHLIP-inserted form, because Asp and Glu residues at the C-terminus of the peptide are deprotonated in the cytoplasm in the environment with a higher intracellular pH. The energy of membrane-associated folding (~2 kcal/mol) could be used to move polar cell-impermeable cargo molecules across the lipid bilayer of the membrane.[8,17,18,26] Our data indicate that the translocation capability could be tuned by conjugating amanitin to the C-terminus of pHLIP via more or fewer hydrophobic linkers. We found that pHLIP-SPDP-amanitin exhibits the most favorable properties, demonstrating 4–5 times higher anti-proliferative ability at pH 6 than at pH 7.4. The major mechanism of amanitin delivery is direct translocation across the membrane by pHLIP and cleavage of the S–S bond in the cytoplasm. Amanitin conjugated to pHLIP via a noncleavable cross-linker was not able to induce cell death. An antiproliferative effect was observed on four different human cancer cell lines. Most cells undergo necrosis, and cell death was observed 40–50 h after treatment. The cytotoxic effect was achieved as the result of cell treatment for 2 h with the pHLIP-amanitin construct at concentrations of 0.25–1 μM. It could be very favorable for in vivo delivery, where the blood flow is significant and small therapeutic molecules have limited time to accumulate in tumors. We already demonstrated that pHLIP targets acidic solid tumors of various origins with high accuracy and stains the entire tumor mass to the degree that correlates

dx.doi.org/10.1021/bi301647y | *Biochemistry* 2013, 52, 1171–1178

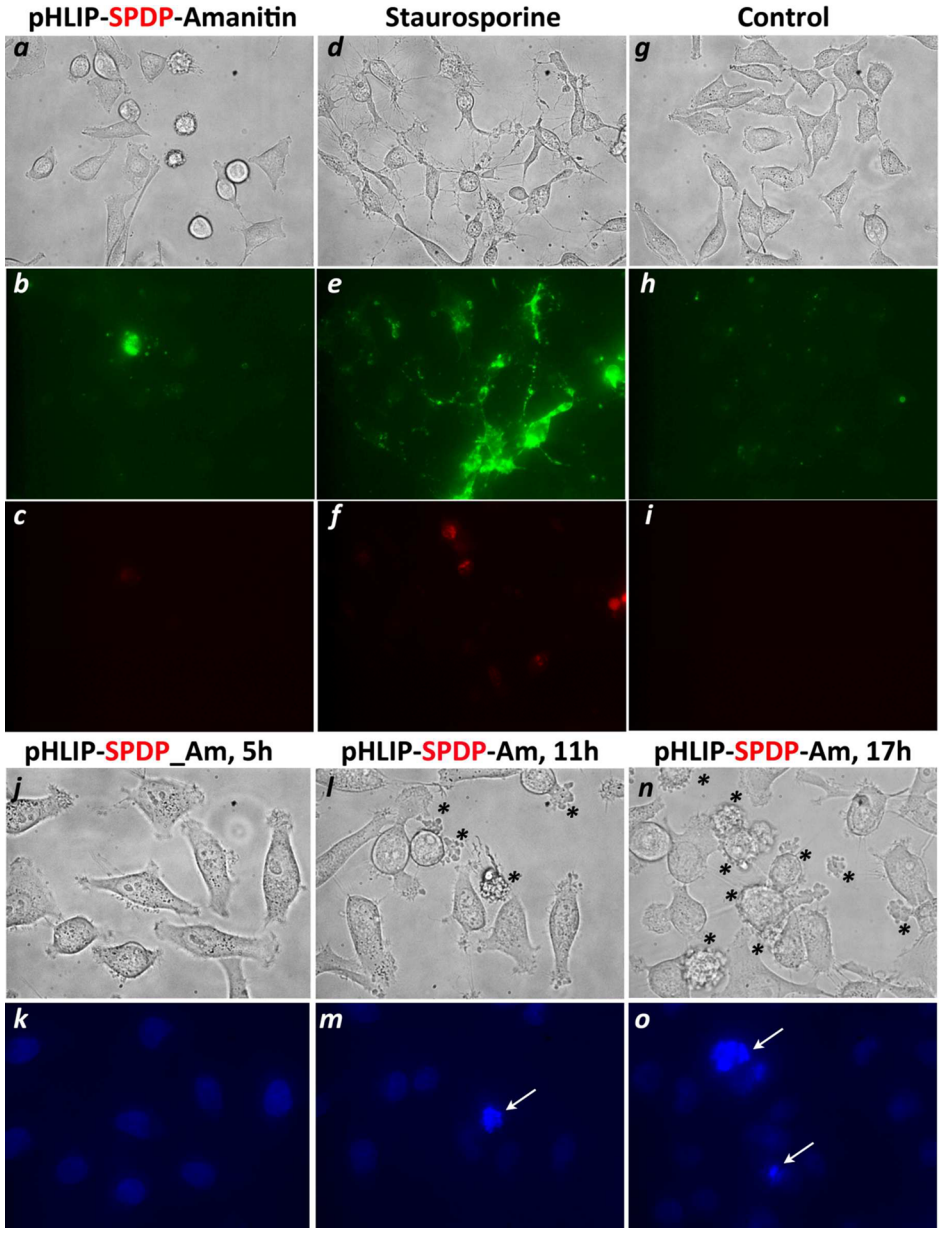

Figure 4. Pathway of cell death. Nontreated HeLa cells (g–i) and cells treated with pHLIP-SPDP-Am (a–c) 11 h after treatment and with staurosporine (d–f) 4 h after treatment were stained with Annexin V-FITC to monitor the appearance of phosphatidylserine at the outer surface of the plasma membrane (b, e, and h) and PI (c, f, and i). The changes in cell morphology (j, l, and n) and DNA fragmentation monitored by staining the cell nucleus with DAPI (k, m, and o) of HeLa cells treated with pHLIP-SPDP-Am were observed 5, 11, and 17 h after the treatment. Only in a small population of cells, which show changes in cell morphology (shown with asterisks), was DNA fragmentation observed (shown with arrows).

with extracellular acidity.[10−12,14,34] Therefore, pHLIP might be effective in the delivery of phallo and amanita toxins to tumors and in their translocation across the membrane of cancer cells with a low extracellular pH and a reverse pH gradient. Amanitin will be most effective in killing highly proliferative cancer cells, which actively synthesize proteins. Thus, selective death of cancer cells with a minimal effect on normal cells might be achieved using pHLIP-mediated delivery of phallo and amanita toxins.

AUTHOR INFORMATION

Corresponding Author

*Physics Department, University of Rhode Island, 2 Lippitt Rd., Kingston, RI 02881. Phone: (401) 874-2060. Fax: (401) 874-2380. E-mail: reshetnyak@mail.uri.edu.

Funding

The work was supported by National Institutes of Health Grant CA133890 to O.A.A. and Y.K.R. The work of V.M. was supported partially by the James Monroe summer research fellowship.

Notes

The authors declare no competing financial interest.

ACKNOWLEDGMENTS

We are grateful to Mr. D. Weerakkody (University of Rhode Island) and Dr. A. Karabadzhak (Yale University) for the assistance with the biophysical measurements. Mass spectrometry was conducted at the RI-INBRE core facility funded by National Center for Research Resources Grant P20RR016457.

■ ABBREVIATIONS

AC, alternating; Am, amanitin; AMAS, *N*-(α-maleimidoacetoxy)succinimide ester; CCD, charged coupled device; CD, circular dichroism; DAPI, 4′,6-diamidino-2-phenylindole; DMEM, Dulbecco's modified Eagle's medium; ECIS, electric cell−substrate impedance sensing; EpCAM, epithelial cell adhesion molecule; FBS, fetal bovine serum; FITC, fluorescein isothiocyanate; HPLC, high-pressure liquid chromatography; OD, optical density; PET, positron emission tomography; PFAST, protein fluorescence and structural database; pHLIP, pH low insertion peptide; PI, propidium iodide; POPC, 1-palmitoyl-2-oleoyl-*sn*-glycero-3-phosphocholine; SELDI-TOF, surface-enhanced laser desorption ionization time-of-flight; SFX, 6-(fluorescein-5-carboxamido)hexanoic acid, succinimidyl ester; SPDP, *N*-succinimidyl 3-(2-pyridyldithio)propionate; SPECT, single-photon emission tomography; sulfo-Lc-SMPT, succinimidyl 6-[α-methyl-α-(2-pyridyldithio)toluamido]hexanoate.

■ REFERENCES

(1) Torchilin, V. P. (2010) Passive and active drug targeting: Drug delivery to tumors as an example. *Handb. Exp. Pharmacol.*, 3−53.

(2) Cheng, Z., Al Zaki, A., Hui, J. Z., Muzykantov, V. R., and Tsourkas, A. (2012) Multifunctional nanoparticles: Cost versus benefit of adding targeting and imaging capabilities. *Science 338*, 903−910.

(3) Boomer, J. A., Qualls, M. M., Inerowicz, H. D., Haynes, R. H., Patri, V. S., Kim, J. M., and Thompson, D. H. (2009) Cytoplasmic delivery of liposomal contents mediated by an acid-labile cholesterol-vinyl ether-PEG conjugate. *Bioconjugate Chem. 20*, 47−59.

(4) Fattal, E., Couvreur, P., and Dubernet, C. (2004) "Smart" delivery of antisense oligonucleotides by anionic pH-sensitive liposomes. *Adv. Drug Delivery Rev. 56*, 931−946.

(5) Guo, X., and Szoka, F. C., Jr. (2001) Steric stabilization of fusogenic liposomes by a low-pH sensitive PEG−diortho ester−lipid conjugate. *Bioconjugate Chem. 12*, 291−300.

(6) Simoes, S., Moreira, J. N., Fonseca, C., Duzgunes, N., and de Lima, M. C. (2004) On the formulation of pH-sensitive liposomes with long circulation times. *Adv. Drug Delivery Rev. 56*, 947−965.

(7) Turk, M. J., Reddy, J. A., Chmielewski, J. A., and Low, P. S. (2002) Characterization of a novel pH-sensitive peptide that enhances drug release from folate-targeted liposomes at endosomal pHs. *Biochim. Biophys. Acta 1559*, 56−68.

(8) Reshetnyak, Y. K., Andreev, O. A., Lehnert, U., and Engelman, D. M. (2006) Translocation of molecules into cells by pH-dependent insertion of a transmembrane helix. *Proc. Natl. Acad. Sci. U.S.A. 103*, 6460−6465.

(9) Andreev, O. A., Dupuy, A. D., Segala, M., Sandugu, S., Serra, D. A., Chichester, C. O., Engelman, D. M., and Reshetnyak, Y. K. (2007) Mechanism and uses of a membrane peptide that targets tumors and other acidic tissues in vivo. *Proc. Natl. Acad. Sci. U.S.A. 104*, 7893−7898.

(10) Daumar, P., Wanger-Baumann, C. A., Pillarsetty, N., Fabrizio, L., Carlin, S. D., Andreev, O. A., Reshetnyak, Y. K., and Lewis, J. S. (2012) Efficient ^{18}F-Labeling of Large 37-Amino-Acid pHLIP Peptide Analogues and Their Biological Evaluation. *Bioconjugate Chem. 23*, 1557−1566.

(11) Macholl, S., Morrison, M. S., Iveson, P., Arbo, B. E., Andreev, O. A., Reshetnyak, Y. K., Engelman, D. M., and Johannesen, E. (2012) In vivo pH imaging with ^{99m}Tc-pHLIP. *Molecular Imaging and Biology 14*, 725−734.

(12) Reshetnyak, Y. K., Yao, L., Zheng, S., Kuznetsov, S., Engelman, D. M., and Andreev, O. A. (2011) Measuring tumor aggressiveness and targeting metastatic lesions with fluorescent pHLIP. *Molecular Imaging Biology 13*, 1146−1156.

(13) Davies, A., Lewis, D. J., Watson, S. P., Thomas, S. G., and Pikramenou, Z. (2012) pH-controlled delivery of luminescent europium coated nanoparticles into platelets. *Proc. Natl. Acad. Sci. U.S.A. 109*, 1862−1867.

(14) Vavere, A. L., Biddlecombe, G. B., Spees, W. M., Garbow, J. R., Wijesinghe, D., Andreev, O. A., Engelman, D. M., Reshetnyak, Y. K., and Lewis, J. S. (2009) A novel technology for the imaging of acidic prostate tumors by positron emission tomography. *Cancer Res. 69*, 4510−4516.

(15) Sosunov, E. A., Anyukhovsky, E. P., Sosunov, A. A., Moshnikova, A., Wijesinghe, D., Engelman, D. M., Reshetnyak, Y. K., and Andreev, O. A. (2013) pH (low) insertion peptide (pHLIP) targets ischemic myocardium. *Proc. Natl. Acad. Sci. U.S.A. 110*, 82−86.

(16) Yao, L., Danniels, J., Moshnikova, A., Kuznetsov, S., Ahmed, A., Engelman, D. M., Reshetnyak, Y. K., and Andreev, O. A. (2013) pHLIP peptide targets nanogold particles to tumors. *Proc. Natl. Acad. Sci. U.S.A. 110*, 465−470.

(17) An, M., Wijesinghe, D., Andreev, O. A., Reshetnyak, Y. K., and Engelman, D. M. (2010) pH-(low)-insertion-peptide (pHLIP) translocation of membrane impermeable phalloidin toxin inhibits cancer cell proliferation. *Proc. Natl. Acad. Sci. U.S.A. 107*, 20246−20250.

(18) Wijesinghe, D., Engelman, D. M., Andreev, O. A., and Reshetnyak, Y. K. (2011) Tuning a polar molecule for selective cytoplasmic delivery by a pH (Low) insertion peptide. *Biochemistry 50*, 10215−10222.

(19) Wieland, T., and Faulstich, H. (1978) Amatoxins, phallotoxins, phallolysin, and antamanide: The biologically active components of poisonous *Amanita* mushrooms. *CRC Crit. Rev. Biochem. 5*, 185−260.

(20) Vetter, J. (1998) Toxins of *Amanita phalloides*. *Toxicon 36*, 13−24.

(21) Walton, J. D., Hallen-Adams, H. E., and Luo, H. (2010) Ribosomal biosynthesis of the cyclic peptide toxins of *Amanita* mushrooms. *Biopolymers 94*, 659−664.

(22) Stirpe, F., and Fiume, L. (1967) Effect of α-amanitin on ribonucleic acid synthesis and on ribonucleic acid polymerase in mouse liver. *Biochem. J. 103*, 67P−68P.

(23) Shen, C., Menon, R., Das, D., Bansal, N., Nahar, N., Guduru, N., Jaegle, S., Peckham, J., and Reshetnyak, Y. K. (2008) The protein fluorescence and structural toolkit: Database and programs for the analysis of protein fluorescence and structural data. *Proteins 71*, 1744−1754.

(24) Karabadzhak, A. G., Weerakkody, D., Wijesinghe, D., Thakur, M. S., Engelman, D. M., Andreev, O. A., Markin, V. S., and Reshetnyak, Y. K. (2012) Modulation of the pHLIP Transmembrane Helix Insertion Pathway. *Biophys. J. 102*, 1846−1855.

(25) Reshetnyak, Y. K., Segala, M., Andreev, O. A., and Engelman, D. M. (2007) A monomeric membrane peptide that lives in three worlds: In solution, attached to, and inserted across lipid bilayers. *Biophys. J. 93*, 2363−2372.

(26) Reshetnyak, Y. K., Andreev, O. A., Segala, M., Markin, V. S., and Engelman, D. M. (2008) Energetics of peptide (pHLIP) binding to and folding across a lipid bilayer membrane. *Proc. Natl. Acad. Sci. U.S.A. 105*, 15340−15345.

(27) Wegener, J., Keese, C. R., and Giaever, I. (2000) Electric cell-substrate impedance sensing (ECIS) as a noninvasive means to monitor the kinetics of cell spreading to artificial surfaces. *Exp. Cell Res. 259*, 158−166.

(28) Tafani, M., Minchenko, D. A., Serroni, A., and Farber, J. L. (2001) Induction of the mitochondrial permeability transition mediates the killing of HeLa cells by staurosporine. *Cancer Res. 61*, 2459−2466.

(29) Nicolier, M., Decrion-Barthod, A. Z., Launay, S., Pretet, J. L., and Mougin, C. (2009) Spatiotemporal activation of caspase-dependent and -independent pathways in staurosporine-induced apoptosis of p53wt and p53mt human cervical carcinoma cells. *Biol. Cell 101*, 455−467.

(30) Munter, K., Mayer, D., and Faulstich, H. (1986) Characterization of a transporting system in rat hepatocytes. Studies with competitive and non-competitive inhibitors of phalloidin transport. *Biochim. Biophys. Acta 860*, 91−98.

(31) Moldenhauer, G., Salnikov, A. V., Luttgau, S., Herr, I., Anderl, J., and Faulstich, H. (2012) Therapeutic potential of amanitin-conjugated anti-epithelial cell adhesion molecule monoclonal antibody against pancreatic carcinoma. *J. Natl. Cancer Inst. 104*, 622−634.
(32) Kozin, S. V., Shkarin, P., and Gerweck, L. E. (2001) The cell transmembrane pH gradient in tumors enhances cytotoxicity of specific weak acid chemotherapeutics. *Cancer Res. 61*, 4740−4743.
(33) Raghunand, N., Altbach, M. I., van Sluis, R., Baggett, B., Taylor, C. W., Bhujwalla, Z. M., and Gillies, R. J. (1999) Plasmalemmal pH-gradients in drug-sensitive and drug-resistant MCF-7 human breast carcinoma xenografts measured by ^{31}P magnetic resonance spectroscopy. *Biochem. Pharmacol. 57*, 309−312.
(34) Segala, J., Engelman, D. M., Reshetnyak, Y. K., and Andreev, O. A. (2009) Accurate Analysis of Tumor Margins Using a Fluorescent pH Low Insertion Peptide (pHLIP). *Int. J. Mol. Sci. 10*, 3478−3487.